Isotopic anomaly and stratification of Ca in magnetic Ap stars⋆

T. Ryabchikova[1,2], O. Kochukhov[3], and S. Bagnulo[4]

[1] Department of Astronomy, University of Vienna, Türkenschanzstraße 17, 1180 Vienna, Austria
[2] Institute of Astronomy, Russian Academy of Sciences, Pyatnitskaya 48, 109017 Moscow, Russia
[3] Department of Physics and Astronomy, Uppsala University, SE-751 20, Uppsala, Sweden
[4] Armagh Observatory, College Hill, Armagh BT61 9DG, Northern Ireland

Received / Accepted

ABSTRACT

Aims. We have carried out an accurate investigation of the Ca isotopic composition and stratification in the atmospheres of 23 magnetic chemically peculiar (Ap) stars of different temperature and magnetic field strength.
Methods. With the UVES spectrograph at the 8 m ESO VLT, we have obtained high-resolution spectra of Ap stars in the wavelength range 3000–10000 Å. Using a detailed spectrum synthesis calculations, we have reproduced a variety of Ca lines in the optical and ultraviolet spectral regions, inferring the overall vertical distribution of Ca abundance, then we have deduced the relative isotopic composition and its dependence on height using the profile of the the IR-triplet Ca II line at λ 8498 Å.
Results. In 22 out of 23 studied stars, we found that Ca is strongly stratified, being usually overabundant by 1.0–1.5 dex below $\log\tau_{5000} \approx -1$, and strongly depleted above $\log\tau_{5000} = -1.5$. The IR-triplet Ca II line at λ 8498 Å reveals a significant contribution of the heavy isotopes ^{46}Ca and ^{48}Ca, which represent less than 1 % of the terrestrial Ca isotopic mixture. We confirm our previous finding that the presence of heavy Ca isotopes is generally anticorrelated with the magnetic field strength. Moreover, we discover that in Ap stars with relatively small surface magnetic fields ($\leq$ 4–5 kG), the light isotope ^{40}Ca is concentrated close to the photosphere, while the heavy isotopes are dominant in the outer atmospheric layers. This vertical isotopic separation, observed for the first time for any metal in a stellar atmosphere, disappears in stars with magnetic field strength above 6–7 kG.
Conclusions. We suggest that the overall Ca stratification and depth-dependent isotopic anomaly observed in Ap stars may be attributed to a combined action of the radiatively-driven diffusion and light-induced drift.

Key words. stars: abundances – stars: atmospheres – stars: chemically peculiar – stars: magnetic fields

1. Introduction

After the pioneering work by Michaud (1970), atomic diffusion in stellar envelopes and atmospheres has been recognized as the main process responsible for the atmospheric abundance anomalies in the peculiar stars of the upper main sequence. Due to their unique characteristics, such as an extremely slow rotation, strong, global magnetic fields, and the absence of convective mixing, magnetic chemically peculiar (Ap and Bp) stars exhibit the most clear manifestation of diffusion effects and thus represent privileged laboratories for investigation of chemical transport processes and magnetohydrodynamics.

Detailed diffusion calculations performed for a set of chemical elements in the atmospheres of magnetic peculiar stars predict separation of chemical elements over the stellar surface and with height in stellar atmosphere (abundance stratification). These theoretical predictions can be directly tested through the comparison with empirical maps of chemical elements inferred from observations. For a small number of elements, including Ca, an effect of the vertically stratified element distribution on the spectral line profiles was demonstrated in early studies (Borsenberger at al. 1981). However, the absence of high-resolution, high signal-to-noise spectroscopic observations did not allow a robust comparison between observations and theoretical diffusion modelling. This step was carried out by Babel (1992), who calculated the Ca abundance distribution in the atmosphere of magnetic Ap star 53 Cam and showed that the unusual shape of Ca II K line – a combination of the wide wings and extremely narrow core (Babel 1994; Cowley et al. 2006) – is a result of a step-like Ca distribution with abundance decrease at $\log\tau_{5000} \approx -1$. Following Babel, the step-function approximation for the abundance distributions was employed in many stratification studies based on the observed profiles of spectral lines (Savanov et al. 2001; Bagnulo et al. 2001; Wade et al. 2003; Ryabchikova et al. 2002, 2005, 2006; Glagolevskii et al. 2005; Cowley et al. 2007).

Ca was found to be stratified in nearly the same way as in 53 Cam (enhanced concentration of Ca below $\log\tau_{5000} \approx -1$ and its depletion above this level) in all stars for which stratification analysis have been performed: β CrB (Wade et al. 2003), γ Equ (Ryabchikova et al. 2002), HD 204411 (Ryabchikova et al. 2005), HD 133792 (Kochukhov et al. 2006a) and HD 144897 (Ryabchikova et al. 2006). In addition to remarkable diffusion signatures, recently another Ca anomaly was detected, first in the spectra of the Hg-Mn stars by Castelli & Hubrig (2004) and then in Ap stars by Cowley & Hubrig (2005). These authors found a displacement of the lines of Ca II IR triplet due to significant contribution of the heavy Ca isotopes. Ryabchikova, Kochukhov & Bagnulo (see review paper by Ryabchikova (2005)) were the first to apply spectrum synthesis calculations to investigate effects of Ca isotopes on the calcium line profile shape in magnetic CP stars. In particular, we have demonstrated the general anticor-

Send offprint requests to: T. Ryabchikova,
e-mail: ryabchik@inasan.ru

⋆ Based on observations collected at the European Southern Observatory, Paranal, Chile (ESO program No. 68.D-0254)

relation between the presence of heavy Ca and magnetic field strength: in Ap stars the contribution of heavy Ca isotopes decreases with the increase of the field modulus, and disappears when the field strength exceeds ∼ 3 kG. Cowley et al. (2007) have come to a similar conclusion, but with reservations.

In the present paper we summarise our detailed analysis of the vertical stratification of Ca abundance in the atmospheres of magnetic Ap stars of different temperatures and magnetic field strengths. We combine this vertical Ca mapping with the analysis of the Ca isotopic anomaly and its dependence on height, based on the spectrum synthesis modelling of the IR triplet Ca II line at λ 8498 Å. Our study is the first to present a homogeneous and systematic determination of the vertical stratification of a given element in the atmospheres of a large number of stars, enabling us to study the signatures of atmospheric atomic diffusion in the presence of strong magnetic field as a function of stellar parameters and magnetic field intensity.

Our paper is organized as follows. In Sect. 2 we describe spectroscopic observations and the data reduction. Determination of the stellar atmospheric parameters is detailed in Sect. 3. Sects. 4–6 present our methodological approach to magnetic spectrum synthesis, determination of Ca stratification and the study of Ca isotopic composition. Our findings are summarised in Sect. 7 and are discussed in Sect. 8.

2. Observations and data reduction

Twenty-three slowly rotating Ap stars were chosen for the Ca stratification analysis. The list of program stars is given in Table 1. In addition, three stars, Procyon (=HD 61421, spectral type F5), HD 27411 (=HIP 20106, spectral type A3m), and HD 73666 (=40 Cnc, spectral type A1 V) were used as standards for the Ca isotopic study. Of the 23 magnetic Ap stars included in our study, 12 stars show high-overtone acoustic *p*-mode pulsations and thus belong to the group of rapidly oscillating Ap (roAp) stars.

We note that metallic line stars show signatures of strong turbulence and convection in their atmospheres (Landstreet 1998; Kochukhov et al. 2006b). Theoretical diffusion models for Am stars (e.g. Michaud et al. 2005) achieve reasonable success in reproducing the surface abundance patterns assuming full mixing of the outer envelope. Thus, despite non-solar abundances, strong mixing inhibits development of the vertical chemical gradients in the line-forming region and for this reason Am star HD 27411 can be considered as a comparison object in the context of the present investigation.

For the majority of our targets high-resolution, high signal-to-noise-ratio spectra were obtained with the UVES instrument (Dekker et al. 2000) at the ESO VLT in the context of program 68.D-0254. The observations were carried out using both available dichroic modes (standard settings 346+580 nm and 437+860 nm). In both the blue arm and the red arm the slit width was set to 0.5″, for a spectral resolution of about 80 000. The slit was oriented along the parallactic angle, in order to minimize losses due to atmospheric dispersion. Almost the full wavelength interval from 3030 to 10400 Å was observed except for a few gaps, the largest of which was at 5760–5835 Å and 8550–8650 Å. In addition, there are several small gaps, about 1 nm each, due to the lack of overlapping between the échelle orders in the 860U setting.

Spectra of HD 24712 and HD 61421 (Procyon) were acquired with the UVES at VLT as part of the UVESpop project[1] (Bagnulo et al. 2003a). The UVES observations of the magnetic Ap star HD 66318 employed in our paper were described by Bagnulo et al. (2003b). All three stars were observed using the same instrumental settings as the Ap targets from our main data set. Spectrum of HD 73666 was obtained with the ESPaDOnS spectropolarimeter at the Canada-France-Hawaii Telescope and analysed for abundances by Fossati et al. (2007). A reduced spectrum was kindly provided to us by the authors.

The UVES spectra have been reduced with the automatic pipeline described in Ballester et al. (2000). For all settings, science frames are bias-subtracted and divided by the extracted flat-field, except for the 860 nm setting, where the 2-D (pixel-to-pixel) flat-fielding is used, in order to better correct for the fringing. Because of the high flux of the spectra, we used the UVES pipeline *average extraction* method.

Due to the gaps in spectral coverage, only one line of the Ca II IR triplet, λ 8498 Å, could be observed in all stars and is accessible for modelling. This line is the weakest among the three IR triplet transitions, which facilitates quantitative analysis, especially in cooler stars where the triplet Ca II lines become particularly strong.

All three lines of the Ca II IR triplet overlap with the hydrogen Paschen lines, which become very prominent in the spectra of hotter Ap stars (see Fig. 1). The 8498 Å line is located further away from the centre of the nearest Paschen line (P16) than the other two lines of the IR triplet. The hydrogen line blending for this Ca II transition is also weaker than for the other two Ca II lines. Moreover, being the weakest among three IR triplet lines the 8498 Å line is less dependent on the accuracy of Stark and Van der Waals broadening parameters. These circumstances suggest the Ca II 8498 Å line is most suitable for detailed modelling.

The studied Ca II line lies rather close to the gap in the wavelength coverage of the UVES setting employed. An additional difficulty arises due to the broad overlapping absorption produced by the Paschen lines. These properties of the data complicate continuum normalization in the region around Ca II 8498 Å. In fact, with the available data, we are generally unable to rectify the spectra in the usual manner. Instead, for each star observations were adjusted to match calculated Paschen line spectrum in a small region around the P16 line. This procedure was carried out in two steps. First, a high-order spline function was employed to trace the wings of the hydrogen line, and observations were divided by this fit. Secondly, observed spectra were multiplied by the theoretical hydrogen line spectrum calculated using individual stellar atmospheric parameters and hydrogen line opacity described in Sect. 4.

For most program stars spectral coverage of our UVES spectra precluded analysis of the two stronger lines of the IR triplet, Ca II 8542 and 8662 Å. However, for one of the targets, HD 24712, we have investigated these lines using complimentary observations obtained with the ESPaDOnS instrument at CFHT. The ESPaDOnS spectrum HD 24712 is the average of 81 time-resolved observations of this star analysed by Kochukhov & Wade (2007). We refer to this paper for the details of reduction of these data. Unlike the UVES spectrum of HD 24712, the ESPaDOnS data were collected close to the phase of magnetic maximum (JD 2453744.71–2453744.83).

3. Fundamental stellar parameters

Fundamental parameters of the program stars are given in Table 1. For most stars effective temperatures $T_{\rm eff}$ and surface gravities $\log g$ were taken from the recent studies (references are

[1] http://www.eso.org/uvespop/

Table 1. Fundamental parameters of the program stars. The columns give the target HD number, range of Julian dates of its observation with UVES, effective temperature, surface gravity, projected rotational velocity, estimate of the mean magnetic field modulus and the ratio of radial to azimuthal field strength adopted in spectrum synthesis. Rapidly oscillating Ap (roAp) stars are identified by asterisk.

HD number	JD−2450000	$T_{\rm eff}$ (K)	$\log g$	$v_{\rm e}\sin i$ (km s^{-1})	$\langle B_{\rm s}\rangle$ (kG)	$B_{\rm r}/B_{\rm a}$	Reference
Magnetic chemically peculiar stars							
965	2190.632–2190.646	7500	4.00	3.0	4.4	3.2/3.2	RKP
24712*	1982.545–1982.561	7250	4.30	5.6	2.3	2.3/0.0	RLG97
29578	2213.805–2213.819	7800	4.20	2.5	5.6	4.5/3.4	RNW04
47103	2286.690–2286.719	8180	3.50	0.0	16.3	0.0/16.3	RKP
66318	2413.467–2413.477	9200	4.25	0.0	15.5	10.2/11.7	BLL03
75445	2236.837–2236.846	7650	4.00	3.0	3.0	2.8/1.0	RNW04
101065*	2280.849–2280.863	6600	4.20	3.5	2.3	2.3/0.0	CRK00
111133	2294.861–2294.866	9930	3.65	5.0	4.0	4.0/0.0	RKP
116114*	2296.864–2296.871	8000	4.10	2.5	6.2	4.6/3.9	RNW04
118022	2298.861–2298.865	9500	4.00	10.0	3.0	3.0/0.0	RKP
122970*	2295.862–2295.875	6930	4.10	5.5	2.5	2.5/0.0	RSH00
128898*	2320.870–2320.873	7900	4.20	12.5	1.5	1.5/0.0	KRW96
133792	2331.791–2331.797	9400	3.70	0.0	1.1	1.1/0.0	KTR06
134214*	2331.816–2331.826	7315	4.45	2.0	3.1	2.5/1.7	RKP
137909*	2331.892–2331.895	8000	4.30	2.5	5.4	5.0/2.0	RNW04
137949*	2331.803–2331.810	7550	4.30	1.0	5.0	2.2/4.5	RNW04
144897	2331.834–2331.851	11250	3.70	3.0	8.8	6.3/6.2	RRK06
166473*	2189.508–2189.517	7700	4.20	0.0	8.6	5.0/7.0	GRW00
170973	2190.511–2190.518	10750	3.50	8.0	0.0		K03
176232*	2190.522–2190.528	7650	4.00	2.0	1.5	1.5/0.0	RSH00
188041	2190.599–2190.605	8800	4.00	0.0	3.6	3.4/1.0	RLK04
203932*	2189.540–2189.557	7550	4.34	5.3	≤1		GKW97
217522*	2189.567–2189.577	6750	4.30	2.5	≤1.5	1.5/0.0	G98
Comparison stars							
27411	2501.937–2501.946	7650	4.00	18.5	0.0		RKP
61421	2555.906–2555.909	6510	3.96	3.5	0.0		AAG02
73666	3745.063–3745.082	9382	3.78	10.0	0.0		FBM07

References. RKP – this paper; RLG97 – Ryabchikova et al. (1997); RNW04 – Ryabchikova et al. (2004b); BLL03 – Bagnulo et al. (2003b); CRK00 – Cowley et al. (2000); RSH00 – Ryabchikova et al. (2000); KRW96 – Kupka et al. (1996); KTR06 – Kochukhov et al. (2006a); RRK06 – Ryabchikova et al. (2006); GRW00 – Gelbmann et al. (2000); K03 – Kato (2003); RLK04 – Ryabchikova et al. (2004a); GKW97 – Gelbmann et al (1997); G98 – Gelbmann (1998); AAG02 – Allende Prieto et al. (2002); FBM07 – Fossati et al. (2007).

provided in the last column of Table 1). For HD 965, HD 47103, HD 118022 and HD 134214 atmospheric parameters were derived using the Strömgren photometric indices extracted from the catalogue of Hauck & Mermilliod (1998). We used calibrations by Moon & Dworetsky (1985) and by Napiwotzki et al. (1993) as implemented in the `TEMPLOGG` code (Rogers 1995). For HD 111133 the effective temperature was taken from Kochukhov & Bagnulo (2006), while other parameters were derived in the present study. For HD 75445, HD 176232 and HD 203932 effective temperatures were further refined by fitting the Hα profile. This resulted in a small correction relative to the published $T_{\rm eff}$ values.

The mean surface magnetic fields $\langle B_{\rm s}\rangle$ were derived using spectral lines which exhibit resolved and partially resolved Zeeman splitting patterns. In all stars rotational velocities were estimated by modelling profiles of the magnetically insensitive Fe I lines at $\lambda\lambda$ 5434.5 and 5576.1 Å. Model atmospheres for all program stars were calculated with the `ATLAS9` code (Kurucz 1993), employing opacity distribution functions (ODFs) with an enhanced metallicity. For stars with especially strong magnetic fields we used ODFs with a non-zero pseudo-microturbulence velocity in order to simulate the modification of the line opacity due to magnetic intensification of spectral lines. All spectrum synthesis for magnetic stars employed zero microturbulence. For comparison stars we have adopted the following values: $\xi_{\rm t} = 1.8$ km s^{-1} for Procyon (Allende Prieto et al. 2002), 1.9 km s^{-1} for HD 73666 (Fossati et al. 2007) and 2.5 km s^{-1} for HD 24711 (determined in this paper).

4. Spectrum synthesis calculations

Analysis of the Ca stratification and isotopic composition was based on detailed magnetic spectrum synthesis calculations with the `SYNTHMAG` code (Kochukhov 2007a). This program allows to solve numerically polarized radiative transfer equation and calculate theoretical stellar spectra in four Stokes parameters for the prescribed model atmosphere and vertical distribution of any number of chemical elements. The `SYNTHMAG` calculations performed in this paper are based on a simplified model of the stellar magnetic field topology, characterized by a single value of the field modulus and a homogeneous field distribution over the surface of the star. When rotation broadening is significant or the field is too weak, we assume purely radial field orientation. In other cases the effective field orientation is inferred from the profiles of magnetically sensitive lines and is parameterized with the ratio of the radial to azimuthal field components (see Table 1). Although undoubtedly rather simplified, this magnetic model is quite successful in explaining the shapes of resolved Zeeman split lines in the Stokes I spectra of many Ap stars (Kochukhov et al. 2002; Nielsen & Wahlgren 2002;

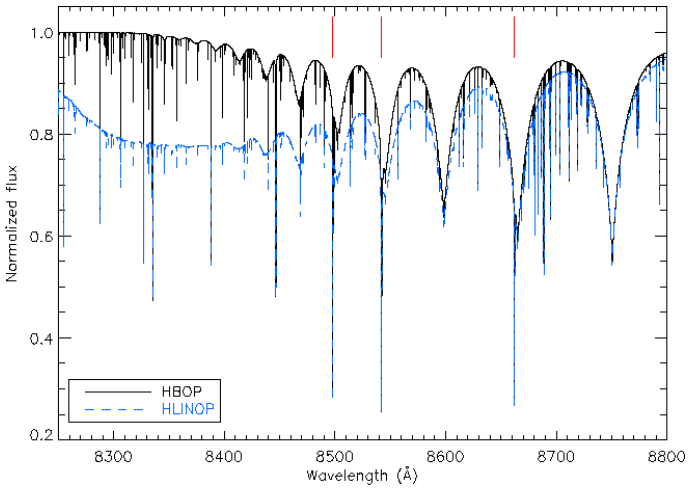

Fig. 1. Synthetic spectra calculated with different treatment of the overlapping hydrogen line opacity. Usual calculation (HLINOP routine, dashed line) is compared with spectrum synthesis based on the occupation probability formalism (HBOP routine, solid line). In both cases ATLAS9 model atmosphere with $T_{\rm eff} = 8500$ K, and $\log g = 4.0$ was adopted. The vertical bars show position of the Ca II IR triplet lines.

Leone et al. 2003; Ryabchikova et al. 2006) and, in some cases, performs even better than low-order multipolar field geometries (Kochukhov 2007b).

In all spectrum synthesis calculations in this paper we use zero microturbulence because the SYNTHMAG code models magnetic intensification by directly including magnetic field effects in the solution of the polarized radiative transfer equation. The true microturbulence is thought be absent in Ap stars because kG-strength magnetic field is quite efficient in suppressing convective motions.

Here we analyse the target stars assuming a homogeneous distribution of Ca over their surfaces. This assumptions appears to be reasonable given a slow rotation of the majority of the targets. Moreover, no evidence of substantial horizontal Ca abundance gradients exist for any of the studied stars, although many of them were observed at high resolution more than once (e.g., Mathys et al. 1997; Ryabchikova et al. 2004b). The only star from our sample for which the Ca surface inhomogeneity was investigated previously, is HD 24712 (Lüftinger et al. 2007). The full range of the horizontal Ca abundance variation in this star is only 0.2 dex. The resulting effect on Ca the line profiles is negligible compared to the vertical abundance jump of more than 3 dex (see below). We also note that, even if hypothetical high-contrast Ca spots exist on the surface of some of our stars, their effect will be to weight our modelling results to specific surface areas. But none of the potential horizontal inhomogeneity effects can possibly mimic stratification or isotopic anomaly studied here.

An important modification to the SYNTHMAG treatment of the hydrogen line opacity was introduced to improve analysis of the IR Ca II triplet lines. These Ca II transitions blend with the high members of the Paschen series, which become prominent in Ap stars with $T_{\rm eff} \geq 8000$ K. The usual calculation of the overlapping hydrogen line wings, which adds linearly opacities due to bound-free and bound-bound hydrogen opacity, becomes increasingly inaccurate as one approaches the series limit. As illustrated in Fig. 1, this leads to a spurious reduction in calculated fluxes. The correct treatment of the overlapping hydrogen line and continuous opacity should be done according to the occupation probability formalism (Daeppen et al. 1987; Hubeny et al. 1994). This technique was implemented in SYNTHMAG with the help of HBOP procedure, developed by P. Barklem at Uppsala Observatory[2]. This hydrogen opacity code, which also incorporates previous developments in the hydrogen line broadening theory (Stehlé & Hutcheon 1999; Barklem et al. 2000), was applied for the spectrum synthesis of all stars in our sample. Fig. 1 shows that correct treatment of the hydrogen opacity significantly reduces predicted Paschen line absorption at the position of the Ca II 8498 Å line analysed here.

Magnetic spectrum synthesis with SYNTHMAG was coupled with the vertical abundance mapping procedure DDAFIT, described by Kochukhov (2007a) and used previously by Ryabchikova et al. (2005, 2006). This routine provides a graphical and optimization interface to SYNTHMAG, allowing the user to find parameters of a simple stratification model by fitting a large number of spectral lines of a given element.

5. Ca stratification analysis

Before performing detailed study of the IR Ca II λ 8498 Å line profile, one has to derive vertical distribution of Ca abundance in the atmospheres of Ap stars. Without this step, a quantitative analysis of isotopic anomaly is practically impossible because profiles of all strong Ca lines, including the IR triplet, are dramatically affected by the vertical stratification of this element. In all program stars Ca stratification was derived using a set of spectral lines in the optical region, for which no indication on the significant isotopic shifts exists. In this way we decouple stratification analysis from the study of isotopic shifts. At this stage we also avoid using the Ca II 8498 Å line because of the possible sensitivity to the errors in effective temperature due to the special normalization procedure adopted for this line (see Sect. 2).

Atomic parameters of the Ca lines are given in Table 2. Stratification analysis requires high accuracy not only for the oscillator strengths but also for the damping parameters, because Ca has a tendency to be concentrated close to the photospheric layers where the electron density is high. Accurate treatment of damping wings is particularly important for the lines of ionized Ca. For the Ca II lines at $\lambda\lambda$ 3158, 3933, 8248, 8254, 8498, 8912, 8927 Å the Stark damping constants were taken from the paper by Dimitrijević & Sahal-Bréchot (1993), where semi-classical calculations as well as a compilation of the experimental data was presented. For the rest of Ca lines the Stark damping constants calculated by Kurucz (1993) were adopted. The oscillator strengths were taken mostly from the laboratory experiments – these data were thoroughly verified by the recent NLTE analysis of calcium in late-type stars (Mashonkina et al. 2007). Because of the large range in effective temperatures and magnetic field strengths, we could not use the same set of lines for all stars.

The Ca stratification analysis was performed using the step-function approximation of the abundance distribution (for details see, e.g., Ryabchikova et al. 2005). This parameterized model of the vertical stratification is characterized by the upper and lower abundance values, as well as by the position and width of abundance jump. In each star these parameters are constrained by simultaneous fit to the profiles of many lines. These observational data are sufficient to constrain stratification parameters with a good precision.

We start stratification analysis of Ca by computing the optimal homogeneous Ca abundance for a chosen set of spectral

[2] http://www.astro.uu.se/~barklem/hlinop.html

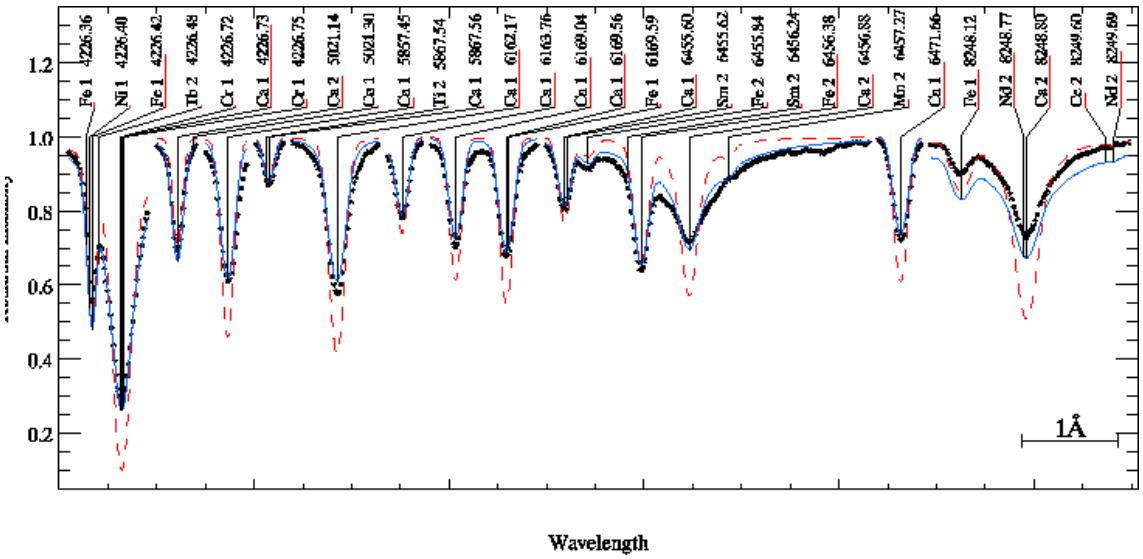

Fig. 2. Comparison between the observed line profiles (symbols) of HD 176232 (10 Aql) and theoretical spectra calculated with the best-fitting stratified Ca abundance distribution (solid line) and with the homogeneous Ca abundance (dashed line). The plotted spectral windows show segments of the HD 176232 spectra used for determination of Ca stratification; symbols show actual observed points.

Table 2. Atomic parameters of the spectral lines employed in the Ca stratification analysis. The columns give the ion designation, central wavelength of the transition, the excitation potential of the lower level, oscillator strength, the Stark damping constant, and the reference for the oscillator strength.

Ion	λ (Å)	E_i (eV)	log gf	log γ_{St}	Reference
Ca II	3158.869	3.123	0.241	−4.90	T
Ca II	3933.655	0.000	0.105	−5.73	T
Ca I	4226.728	0.000	0.244	−6.03	SG
Ca II	5021.138	7.515	−1.207	−4.61	SMP
Ca II	5339.188	8.438	−0.079	−3.70	SMP
Ca I	5857.451	2.933	0.240	−5.42	S
Ca I	5867.562	2.933	−1.570	−4.70	S
Ca I	6122.217	1.896	−0.316	−5.32	SO
Ca I	6162.173	1.899	−0.090	−5.32	SO
Ca I	6163.755	2.521	−1.286	−5.00	SR
Ca I	6166.439	2.521	−1.142	−5.00	SR
Ca I	6169.042	2.253	−0.797	−5.00	SR
Ca I	6169.563	2.256	−0.478	−4.99	SR
Ca I	6449.808	2.521	−0.502	−6.07	SR
Ca I	6455.598	2.523	−1.340	−6.07	S
Ca II	6456.875	8.438	0.410	−3.70	SMP
Ca I	6462.567	2.523	0.262	−6.07	SR
Ca I	6471.662	2.526	−0.686	−6.07	SR
Ca II	8248.796	7.515	0.556	−4.60	SMP
Ca II	8254.721	7.515	−0.398	−4.60	SMP
Ca II	8498.023	1.692	−1.416	−5.70	T
Ca II	8912.068	7.047	0.637	−5.10	SMP
Ca II	8927.356	7.050	0.811	−5.10	SMP

Rerefences. T – Teodosiou (1989); SG – Smith & Gallagher (1966); SMP – Seaton et al. (1994); S – Smith (1988); SO – Smith & O'Neil (1975); SR – Smith & Raggett (1981).

lines. Then we let the DDAFIT procedure to vary parameters of the step-function until the adequate fit to the observed line profiles is achieved. The outcome of this procedure is illustrated in Fig. 2, where results of the stratification analysis for the set of optical lines in HD 176232 (10 Aql) are displayed. Figure 3 shows that stratified Ca distributions obtained for HD 176232 and other cool Ap stars also dramatically improve the fit to the strongest Ca II 3933 Å line compared to the spectrum synthesis with a homogeneous Ca distribution. In Figs. 2 and 3 synthetic profiles calculated with the uniform Ca distribution $\log(Ca/N_{\rm tot}) = -5.14$ are shown by dashed lines while those calculated with the best-fitting stratified Ca distribution are shown by the solid lines. Clearly, even a very schematic Ca stratification model used here provides a substantial improvement of the agreement between observations and theoretical calculations. We use standard deviation to characterize the quality of the fit. This parameter is defined as a rms of the observed minus calculated spectrum, evaluated on the wavelength grid of observations within the spectral windows covering lines of interest (see Fig. 2). For HD 176232 and most other stars the stratified Ca abundance yields roughly two times smaller standard deviation compared to the homogeneous Ca distribution. The final Ca stratification model inferred for HD 176232 is illustrated in Fig. 4.

To verify that the step-function approximation provides a realistic description of the Ca distribution we performed for a few stars with weak magnetic fields (HD 133792, HD 176232, HD 203932) stratification analysis using the Vertical Inverse Problem code, VIP. This program does not use any *a priori* assumptions about the shape of the vertical element abundance profile but currently cannot be applied to stars with a strong magnetic field (Kochukhov et al. 2006a). A comparison between the Ca distributions derived for HD 176232 with DDAFIT and with VIP is shown in Fig. 4. The same level of agreement was obtained for the two other stars.

However, despite general success of the DDAFIT modelling, in a few stars the step-function approximation could not provide an adequate description of the full set of spectral lines. The obvious reason is the use of normal non-magnetic stellar model atmosphere with a homogeneous element distribution for a star with abundance stratification, and a deviation of the Ca abundance distribution from the simple step-function form.

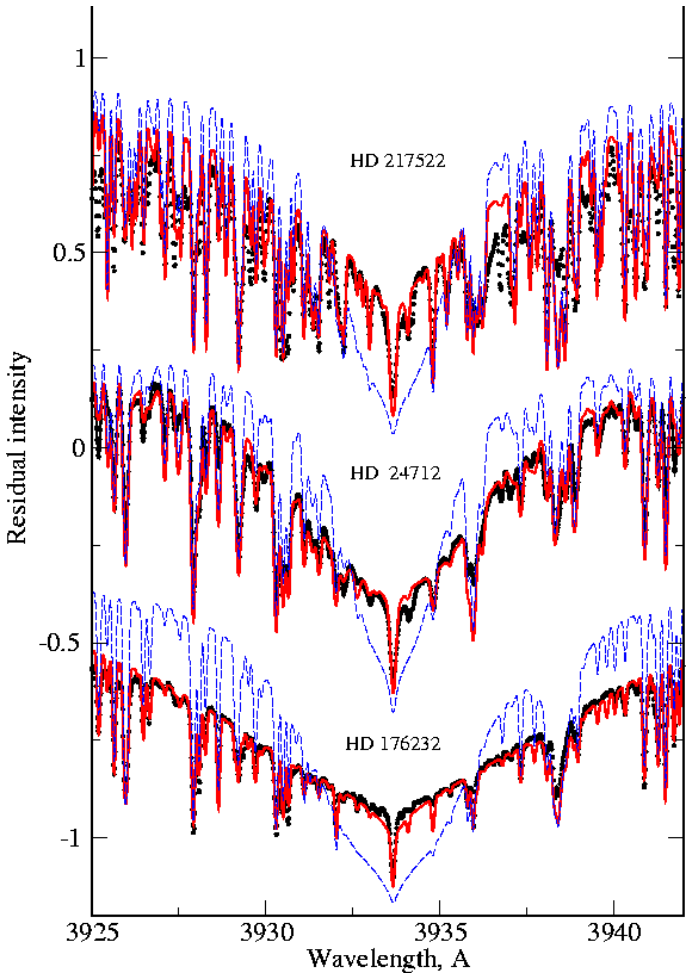

Fig. 3. Comparison between the observed profiles (symbols) of the Ca II 3933 Å line and calculations with the stratified (solid line) and homogeneous (dashed line) Ca distributions for 3 program stars. The spectra of HD 24712 and HD 176232 are shifted downwards for display purpose.

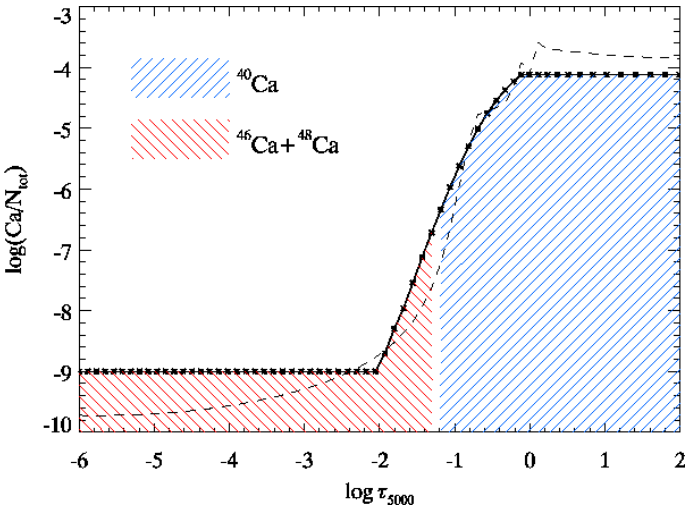

Fig. 4. Vertical stratification and isotopic separation of Ca derived for HD 176232. The overall Ca abundance profile, inferred from the stratification analysis of optical lines, is shown with the solid line. The hatched areas demonstrate vertical separation of the light and heavy Ca isotopes required to fit the Ca II 8498 Å line. The dashed line shows the Ca distribution derived the with VIP code using the same set of lines.

In cooler stars we do not systematically use the strongest Ca II 3933 Å line in the stratification analysis due to difficulties of treating blends in the extended wings and establishing continuum. The range of the formation depths of the remaining weaker optical lines is different from the IR triplet lines of interest, therefore Ca abundance in the upper atmospheric layers is poorly constrained by the optical lines and may not be accurate enough for the description of the cores of the IR Ca II triplet lines. This is often reflected by a rather large formal error of the abundance in the upper layers compared with the corresponding error of the abundance in the lower layers. For several stars (see Table 4) a change of the Ca abundance above in the upper layers within 3σ was introduced to fit overall intensity of the IR triplet line cores. In addition for a few other stars further improvement of the fit quality was possible by introducing a more complicated stratification profile starting from the results obtained with `DDAFIT`. This step was performed manually for 5 out of 23 Ap stars. In all the cases when we have modified Ca stratification determined with `DDAFIT`, the consistency of the altered vertical abundance profile with all Ca diagnostic lines was verified.

The formal stratification analysis of the Am star HD 27411 (whose $T_{\rm eff}$ is identical to that of HD 176232) and normal star HD 73666 ($T_{\rm eff}$=9382 K) yields a 0.2 dex abundance jump, which we consider to be insignificant. The average Ca abundance $\log(\mathrm{Ca}/N_{\rm tot}) = -5.63$ in both stars represents very well most of the lines, including the resonance Ca II 3933 Å line. In both stars 0.1 dex lower abundance is required to fit the Ca II 3933 Å profile compared to Ca II 8498 Å line. This internal agreement is excellent considering difficulties in continuum normalization. It confirms that the Ca abundance variation by several dex over the vertical span of the Ap-star atmospheres is real.

6. The Ca isotopic anomaly

Ca has six stable isotopes with atomic numbers 40, 42, 43, 44, 46, 48. In the terrestrial matter Ca mixture consists mainly of ^{40}Ca (96.9 % according Anders & Grevesse 1989). Table 3 gives wavelengths of all Ca isotopes in the Ca II 8498 Å transition based on the isotopic shifts measured by Nörtershäuser et al. (1998). We also list fractional oscillator strengths corresponding to the terrestrial isotopic mixture.

Isotopic shifts were also measured for the Ca II resonance lines at $\lambda\lambda$ 3933 and 3968 Å (Mårtensson-Pendrill et al. 1992). The wavelength shift between the ^{48}Ca and ^{40}Ca isotopes is −0.009 Å, and can be observed only for the Ca II 3933 Å line core in hot stars with an especially large contribution of the ^{48}Ca isotope. One star from our sample, HD 133792, shows an isotopic shift in the Ca II 3933 Å line.

Using the terrestrial isotopic mixture, we calculated the profile of the Ca II 8498 line in the spectra of our reference stars, Procyon, HD 27411 and HD 73666. Comparison of the theoretical spectra and observations is illustrated in Fig. 5. Although in the Procyon spectrum our LTE calculations cannot provide a very good fit to the deepest part of the core, no wavelength shifts are detected in either star. At the same time, the observed profile of the Ca II line in the spectrum of one of our program stars, HD 217522, presented in Fig. 5 exhibits a complex structure and is clearly redshifted, with the strongest component coinciding in

Table 3. Atomic data for the isotopic components of Ca II λ 8498 Å. The fractional abundance of Ca isotopes, ε, corresponds to the composition of the terrestrial matter.

λ (Å)	isotope	$\log gf\varepsilon$
8498.023	40	−1.43
8498.079	42	−3.60
8498.106	43	−4.29
8498.131	44	−3.10
8498.179	46	−5.81
8498.223	48	−4.14

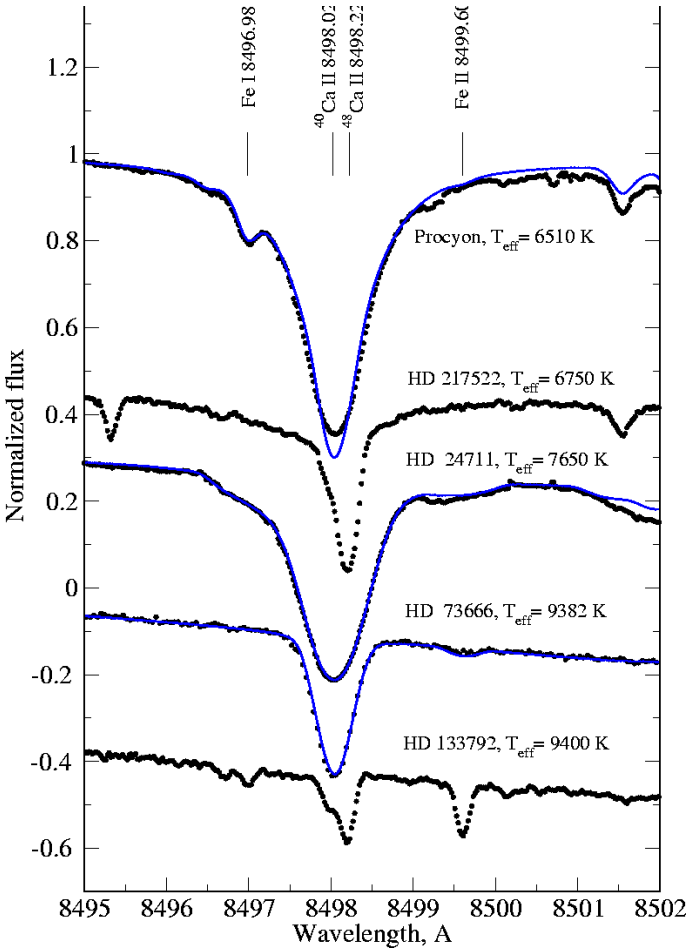

Fig. 5. Comparison between the observed line profiles (symbols) of the Ca II 8498 Å line and calculations for the normal Ca isotopic mixture (solid line) in the spectra of Procyon, Am star HD 27411, and A1 V star HD 73666. The observed spectrum of the cool (HD 217522) and tepid (HD 133792) Ap stars, presented in the middle and bottom, clearly shows a displaced Ca II line core. The spectra are shifted downwards for display purpose.

wavelength with the expected position of the heaviest Ca isotope. This is a signature of the Ca isotopic anomaly and, as we will show below, of the vertical separation of Ca isotopes.

The core of the IR Ca II 8498 Å line is formed higher than any of the optical lines, except Ca II 3933 Å. For most stars the Ca II 3933 Å line was not modelled in our stratification calculations. Therefore, Ca abundance in the upper atmosphere of some stars may be somewhat uncertain, as all other optical lines are not sensitive to the abundance variations above $\log \tau_{5000} = -2.0$

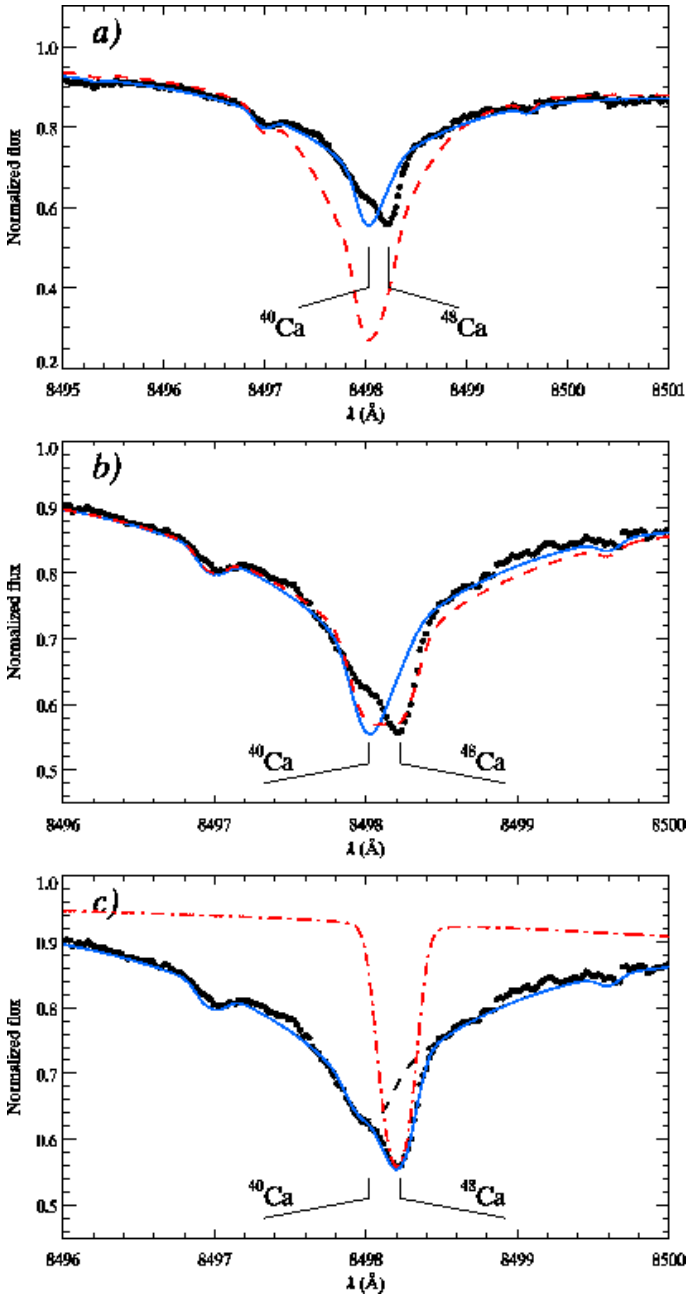

Fig. 6. Derivation of the isotopic composition and its height dependence for the Ca II 8498 Å line in HD 176232 (10 Aql). The three panels show the UVES observations (full circles) compared to various modelling attempts, as follows. **a)** Dashed line: theoretical spectrum obtained with a homogeneous Ca distribution. Solid line: theoretical spectrum calculated for a stratified Ca abundance. A terrestrial mixture of Ca isotopes is adopted for these computations. **b)** Solid line: theoretical spectrum obtained for a terrestrial Ca isotopic composition (same as panel a); Dashed line: theoretical spectrum obtained for a 50:50 ratio of ^{40}Ca to ^{46}Ca+^{48}Ca. **c)** Solid line: the Ca II line profile computed for the best-fitting model of vertical isotopic separation (see Fig. 4). Dashed and dash-dotted lines show contributions of ^{40}Ca and ^{46}Ca+^{48}Ca, respectively. The wavelength position of ^{40}Ca and ^{48}Ca is indicated in each panel. These plots show that an acceptable fit to the observations can only be achieved with a depth-dependent Ca isotopic mixture.

to −2.5. However, for the majority of our targets the Ca abundance in the upper atmosphere, responsible the strength of the Ca II 8498 Å line core, is defined by the slope of the abundance gradient in the jump region. If the Ap atmospheric structure is close to the normal ATLAS9 atmosphere adopted in our analysis, then the Ca II 8498 Å line should be well-described by the Ca abundance distribution derived from optical lines. Our calculations show that while it is correct for the observed total intensity, in many of the program stars we cannot fit the line cores, which are often redshifted. This situation is illustrated in Fig. 6a, where we compare the observed spectrum of HD 176232 with the synthetic spectrum calculated for the terrestrial Ca isotopic mixture and Ca abundance distribution (Fig. 4) derived from optical lines. One immediately notices that while the line wings are explained by our calculations, the line core cannot be fitted with the terrestrial Ca isotopic mixture.

Cowley & Hubrig (2005) showed that the red-shift of the Ca IR line core arises due to the heavy Ca isotopes and claimed that "in extreme cases the dominant isotope is the exotic ^{48}Ca". A simple interpretation of the anomaly observed in the Ca II 8498 Å line core is to suggest that heavy Ca isotopes are strongly enhanced and even dominant throughout the atmospheres of some magnetic Ap stars. However, our magnetic spectrum synthesis calculations demonstrate that this hypothesis is incorrect. On the example of HD 176232 we can show that using a model with stratified Ca distribution found previously and assuming a depth-independent enhancement of ^{46}Ca and ^{48}Ca relative to ^{40}Ca, the center-of-gravity of the Ca II 8498 Å line core is shifted to the red, but the overall fit to the line profile does not improve considerably (Fig. 6b). In disagreement with observations, a constant overabundance of the heavy Ca isotopes gives rise to the red-shifted long-wavelength wing of the Ca II line.

Here we propose a different explanation of the Ca II 8498 Å line shape. Observations of HD 176232 and other stars with displaced Ca line core show a shallow line with wide wings at the position of ^{40}Ca isotope, which means that this line component is formed in the lower atmospheric layers. On the other hand, at the position of ^{48}Ca we see a sharp deep line, which is responsible for a characteristic steep intensity gradient in the red wing of the Ca II 8498 Å line. We observe the same picture in all cool Ap stars with significant isotopic shifts of the Ca II line core. Given the Ca stratification inferred for all Ap stars, this deep component lacking developed wings can be explained by the absorption in the upper atmosphere, above the Ca abundance jump or in the outermost part of the transition region. Thus, observations of the Ca II 8498 Å line in Ap stars should be interpreted in terms of *vertical separation of Ca isotopes in the stellar atmosphere*.

If we separate ^{40}Ca and the sum of ^{46}Ca and ^{48}Ca isotopes in the atmosphere of HD 176232 as indicated in Fig. 4 (the boundary between heavy and light Ca is at $\log \tau_{5000} = -1.2$), a satisfactory agreement between the observed and calculated spectra is obtained (see Fig. 6c). The dominant atmospheric constituent is still the normal isotope ^{40}Ca, but the shape of the Ca II 8498 Å line core is influenced by the high-lying cloud of heavy Ca, in which ^{46}Ca and ^{48}Ca contribute 35% and 65%, respectively.

Thus, in our modelling of the Ca isotopic anomaly in Ap stars we adopt an initial model in which the total element abundance is given by the stratification profile obtained previously, while the vertical separation of the light and heavy Ca isotopes occurs nearly instantaneously and is characterized by a single transition depth, deduced from the Ca II 8498 Å line. Relative contributions of ^{46}Ca and ^{48}Ca to the heavy Ca layer in the upper atmosphere are also adjusted based on the Ca II IR triplet line.

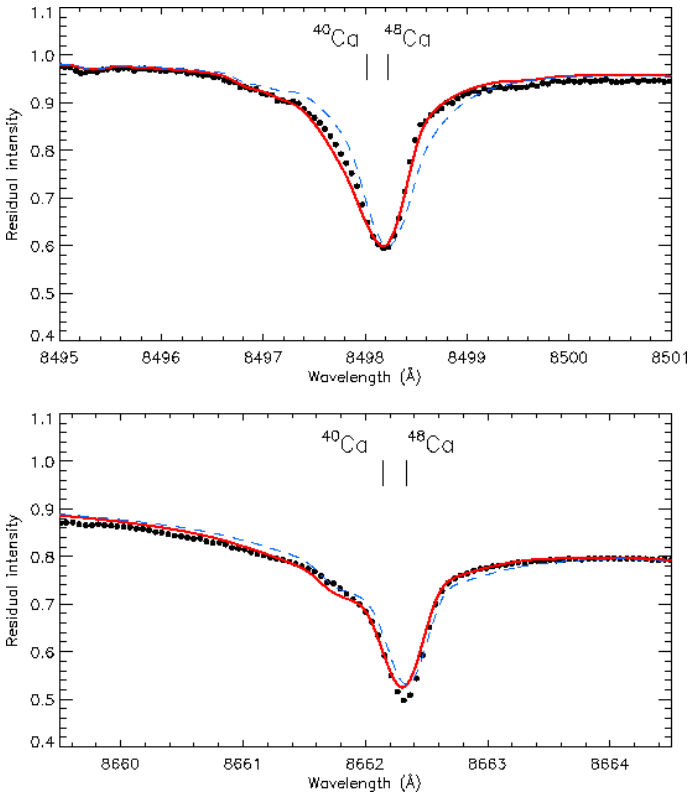

Fig. 7. Comparison of the observed IR triplet lines (symbols) in the ESPaDOnS spectrum of HD 24712 and theoretical spectrum synthesis for the best-fitting stratified Ca abundance distribution (solid line) with Ca isotopic separation and with the stratified distribution of ^{48}Ca only (dashed line).

Parameterization of the vertical separation of Ca isotopes that we adopt here is just one of several models possible. For instance, we find that an acceptable fit to the Ca II 8498 Å line in some of the target stars could be obtained with a model where ^{48}Ca is homogeneously distributed while ^{40}Ca is stratified. (Such a model is achieved by placing the border between Ca isotopes horizontally rather than vertically in Fig. 4. Note, that formally ^{48}Ca is not anomalous: its relative-to-hydrogen abundance in all stars does not exceed an abundance in the normal solar Ca mixture.) This model turns out to be nearly equivalent to the one we use because the boundary between the heavy and light Ca layers is usually located very close to the position of the Ca abundance jump. The ^{40}Ca contribution still dominates in the lower atmosphere, whereas ^{48}Ca contributes to the light absorption in the upper layers. However, for several stars where we need Ca enhancement in the uppermost layers, the model with homogeneously distributed heavy Ca isotopes clearly yields worse agreement with observations in comparison with the vertical separation model adopted in here.

Our isotopic stratification model is based upon only one of the IR triplet lines. High-quality observations of the two other IR triplet lines are unavailable for the majority of our targets. For one of the cool Ap stars, HD 24712, we assessed the quality of the fit to all three Ca II lines using the spectrum obtained with ESPaDOnS at CFHT. These data were collected at the rotational phase different from that of UVES observations, there-

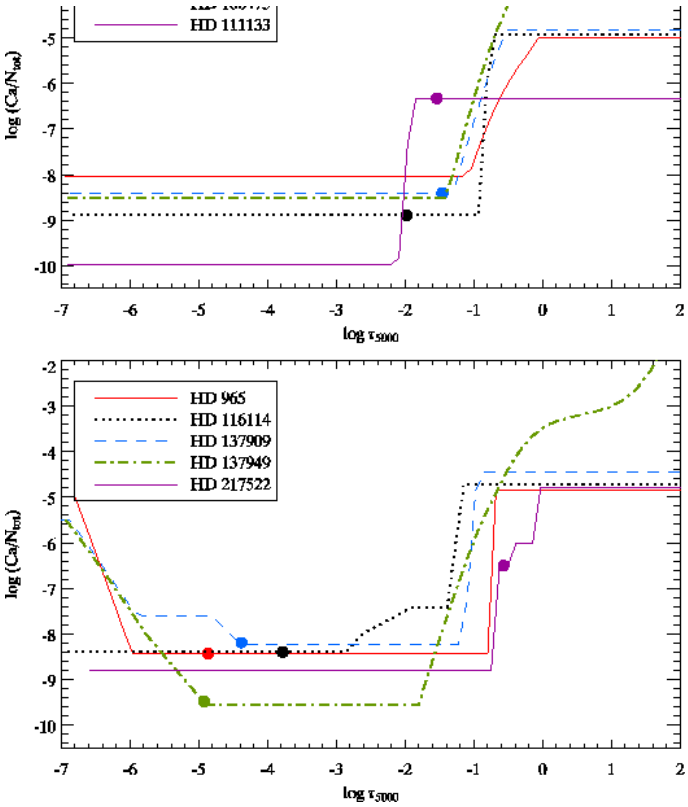

Fig. 8. Ca stratification in the atmospheres of selected program stars. Upper panel: distribution of Ca in HD 66318, HD 75445, HD 134214, HD 166473 and HD 111133. For stars enriched in heavy Ca the filled circle indicates the bottom of the heavy Ca isotope layer. Lower panel: same for stars with complex distribution of Ca abundance with height (HD 965, HD 116114, HD 137909, HD 137949, HD 217522).

fore we have performed an independent Ca stratification and isotopic analysis for HD 24712 based on the ESPaDOnS spectrum alone. Fig. 7 compares calculated and observed Ca II 8498 Å and 8662 Å line profiles. Due to specific position of the Ca II 8542 Å line near the beginning of the spectral order, which makes continuum normalization uncertain, we did not include this line to the plot.

Of course, the proposed model of Ca isotopic separation is at best a crude approximation of potentially much more complex isotopic stratifications. However, we find that, for many stars, introducing a combination of stratification and isotopic segregation noticeably improves the fit to the IR triplet lines and thus provides a direct evidence for the Ca isotopic separation in the atmospheres of Ap stars.

Finally, we note that the continuum normalization in the region around IRT lines is indirectly based on the adopted effective temperatures, which may introduce an additional uncertainty and sometimes lead to a poor fit in the line wings. However, we have verified that even considerable errors in $T_{\rm eff}$ lead only to a small change of the overall depth of the Ca II 8498 Å line computed for a given Ca stratification. Since this line is located far enough from the H line core, its profile, especially the shape of the inner core region used in the isotopic analysis, is generally not affected by the $T_{\rm eff}$ errors.

7. Results

7.1. Ca stratification

The Ca stratification analysis described in Sect. 5 was applied to all Ap stars included in our sample. The presence of a stratified Ca distribution is inferred for all stars except the hot Ap star HD 170973, where stratification appears to be negligible. Table 4 gives parameters of the step-function model distributions of Ca abundance. These vertical abundance profiles are characterized by an abundance jump in the atmospheric region $-1.3 \le \log\tau_{5000} \le -0.5$, a 1–1.5 dex overabundance deep in the atmosphere and a strong Ca depletion above $\log\tau_{5000} \approx -1.5$. The formal uncertainty of the stratification parameters is typically 0.3–0.7 dex, 0.1–0.3 dex and < 0.1 dex for the upper abundance, lower abundance and the position of the Ca abundance jump, respectively. The Ca stratification in the atmospheres of selected program stars is shown in Fig. 8.

For several stars a more complex vertical distributions of Ca abundance had to be introduced. Observations of HD 965, HD 137909, HD 137949 are better reproduced with an increase of Ca concentration in the upper atmospheric layers above $\log\tau_{5000} = -5$. Although seemingly complicated, this picture does not contradict theoretical Ca diffusion calculations. Both Borsenberger et al. (1981, Fig. 6) and Babel (1992) obtained Ca abundance increase in the uppermost layers, above the main abundance jump. However, NLTE treatment of the Ca lines formation is needed to investigate stratification of Ca in the upper atmospheric layers in more detail. For two other stars, HD 116114 and HD 217522, a structure of the transition zone somewhat more complex than a linear transition between two constant values is required to fit observations. Figure 8 (lower panel) illustrates the final chemical stratification profiles adopted for the five stars where Ca stratification deviates from a step-function profile.

We note that for all stars the `DDAFIT` inversion was performed on the original column mass ($\log\rho x$) depth grids of the `ATLAS9` models. Table 4 gives vertical stratification parameters converted to the $\log\tau_{5000}$ scale. In the cases when transition zone is wide, extending to the lower atmospheric layers, transformation between the column mass and the standard optical depth scale becomes non-linear, which leads to a distortion of the step-function shape (e.g., Ca distribution for HD 137949 in Fig. 8). For the same reason in some of the stars where this problem was encountered (e.g., HD 137949, HD 188041) the formal solution for the Ca distribution yields an unrealistically high Ca abundance in the lower atmosphere. However, we find that in these objects the actual inferred stratification profile often has a plateau with $\log(Ca/N_{\rm tot}) \approx -3.5$ in the layers around $\log\tau_{5000} \approx 0$. This value of the abundance gives the actual element concentration that influences the Ca line formation. The formal high Ca abundance occurs far below the photosphere (e.g., the bottom panel of Fig. 8 shows this situation for HD 137949). It does not influence the observed Ca line profiles. Therefore, for all stars marked by a letter '*c*' in Table 4 we took the Ca abundance at $\log\tau_{5000} \approx 0$ as $\log(Ca/N_{\rm tot})_{\rm lo}$, modifying the position and the width of the abundance jump correspondingly.

Homogeneous determination of the calcium vertical distribution in a large number of magnetic Ap stars allows us to search for possible dependence of diffusion signatures on the stellar atmospheric parameters and magnetic field strength. However, except of the marginal tendency of the Ca abundance in the upper layers to be higher in hotter stars, we found no clear correlations between each of the four stratification parameters on the one hand and $T_{\rm eff}$ and $\langle B_{\rm s}\rangle$ on the other hand. Although the

Table 4. Parameters of the Ca stratification and isotopic anomaly determined for magnetic CP stars. The columns give HD number of stars, step-function parameters of the vertical Ca distributions (abundance in upper atmosphere, abundance in the lower layers, position of the abundance jump and the width of the transition zone), parameters of the Ca isotopic separation if applicable (the optical depth of the boundary between the heavy and light Ca layers, the dominant isotopic component of the heavy Ca cloud). The last column indicates deviation of the final Ca stratification profile from a simple step-function.

HD	Stratification parameters				Ca isotopic anomaly		Comment
number	$\log(Ca/N_{\rm tot})_{\rm up}$	$\log(Ca/N_{\rm tot})_{\rm lo}$	$\log\tau_{5000}(step)$	$\Delta\log\tau_{5000}(step)$	$\log\tau_{5000}(isot)$	isotope	
965	−8.4	−4.9	−0.7	0.1	−4.9	^{46}Ca	*a*, *d*
24712	−8.7	−5.1	−1.2	2.5	−1.4	^{46}Ca	*c*, *d*
29578	−8.9	−4.3	−1.2	0.7			
47103	−7.7	−4.6	−0.8	0.3			
66318	−8.0	−5.0	−0.6	1.1			
75445	−8.9	−4.9	−0.9	0.2	−2.0	^{48}Ca	
101065	−8.9	−5.3	−0.4	0.4	−0.2	^{48}Ca	
111133	−10.0	−6.3	−2.0	0.4	−1.5	^{44}Ca	
116114	−7.4	−4.7	−1.3	0.2	−3.8	^{48}Ca	*b*
118022	−7.0	−2.0	−0.1	0.3	−1.5	^{48}Ca	
122970	−7.7	−5.1	−1.5	2.8	−1.6	^{46}Ca	*c*, *d*
128898	−8.5	−4.0	−1.0	2.0	−1.9	^{48}Ca	*c*, *d*
133792	−8.1	−5.6	−0.6	0.1	−1.0	^{48}Ca	
134214	−8.4	−4.8	−0.9	0.9	−1.5	^{48}Ca	
137909	−8.2	−4.4	−1.0	0.4	−4.4	^{48}Ca	*a*
137949	−9.6	−3.5	−1.0	1.8	−4.9	^{48}Ca	*a*, *c*
144897	−8.5	−5.2	−1.9	0.5			
166473	−8.5	−3.8	−1.0	1.1			*d*
170973	−5.3	−5.0	−1.1	0.1			
176232	−9.0	−4.1	−1.2	1.8	−1.2	^{48}Ca	*d*
188041	−7.4	−3.1	−1.2	2.5	−3.7	^{46}Ca	*c*, *d*
203932	−8.7	−4.5	−1.2	2.6	−2.1	^{48}Ca	*c*, *d*
217522	−8.8	−4.8	−0.3	0.7	−0.6	^{48}Ca	*b*

Comments. *a* – abundance increase in the upper layers; *b* – complex transition zone; *c* – distortion of the step-function after $\log\rho x$ to $\log\tau_{5000}$ transformation; *d* – a change in the upper abundance value.

qualitative form of the Ca stratification is the same in all stars, possibly indicating the action of a universal radiative diffusion process, the observed star-to-star variation in stratification profiles appears to be irregular and unrelated to any other stellar characteristic.

7.2. The Ca isotopic anomaly

The Ca isotopic analysis procedure outlined in Sect. 6 was applied to all stars included in our paper. Table 4 lists the lower boundary (uncertain to within ≈ 0.1 dex) of the heavy Ca layer in the atmospheres of magnetic Ap stars for which the Ca II 8498 Å line could not be reproduced with the terrestrial isotopic mixture. Our estimate of the dominant contributor among different heavy Ca isotopes is also given. Out of 23 program stars, the presence of heavy isotopes is established in 17 objects.

For three stars, HD 965, HD 137909, HD 137949, the modelling of the IR triplet line requires an increase of the Ca abundance in the upper atmosphere, above the abundance jump given by the simple stratification analysis. In these cases we attribute the high-lying cloud to heavy Ca.

Figure 9 compares theoretical spectrum synthesis calculations with observations for a subset of 12 cooler ($T_{\rm eff} \le 9000$ K) stars with different effective temperatures and different magnetic field intensity. The stars are arranged in order of increasing magnetic field strength. It is evident that the presence of heavy Ca isotopes inversely correlates with magnetic field strength. This effect is further illustrated in Fig. 11a, where we quantify the detection of heavy Ca by the ratio of calculated equivalent widths of the ^{44}Ca+^{46}Ca+^{48}Ca to ^{40}Ca line components. In the stars with small to moderate magnetic fields we clearly see a significant contribution of the heavy isotopes ^{46}Ca and ^{48}Ca (large equivalent width ratio). This contribution decreases with the increase of magnetic field strength. Even in HD 137909 (β CrB) with the mean magnetic field modulus $\langle B_{\rm s}\rangle = 5.4$ kG one still needs a small contribution of ^{48}Ca, but under the assumption of very specific Ca distribution shown in Fig. 8. No evidence for the presence of heavy Ca is found in cool Ap stars with $\langle B_{\rm s}\rangle \gtrsim 6$ kG.

Due to the temperature dependence of the Ca line intensity, we used a smaller number of lines for stratification analysis of hot Ap stars ($T_{\rm eff} > 9000$ K). In these stars stratification is defined mainly by the Ca II lines. Among the neutral Ca lines only the resonance Ca I 4227 Å line could be utilized. The agreement of calculated and observed line profiles is poorer for hot stars. However, the general anticorrelation between the presence of the heavy Ca isotopes and magnetic field strength is still apparent (see Fig. 10). As in cool stars, no evidence for the presence of heavy Ca is found in hot Ap stars with $\langle B_{\rm s}\rangle \gtrsim 6$ kG. The only exception is HD 170973, which has no observable magnetic field and shows no contribution of the heavy Ca isotopes. We note that HD 170973 is also the only star for which we find no evidence of Ca stratification. This star also possesses the highest Ca abundance among the hot Ap stars in our sample.

Thus, it appears that the mechanism responsible for the accumulation of heavy Ca isotopes in the line-forming atmospheric region works more efficiently in stars with a small magnetic field strength. Figure 11 illustrates several other interesting relations between the Ca isotopic anomaly and stellar parameters that we have revealed in this study. The optical depth of the layer separating the heavy and light Ca clouds depends on the magnetic

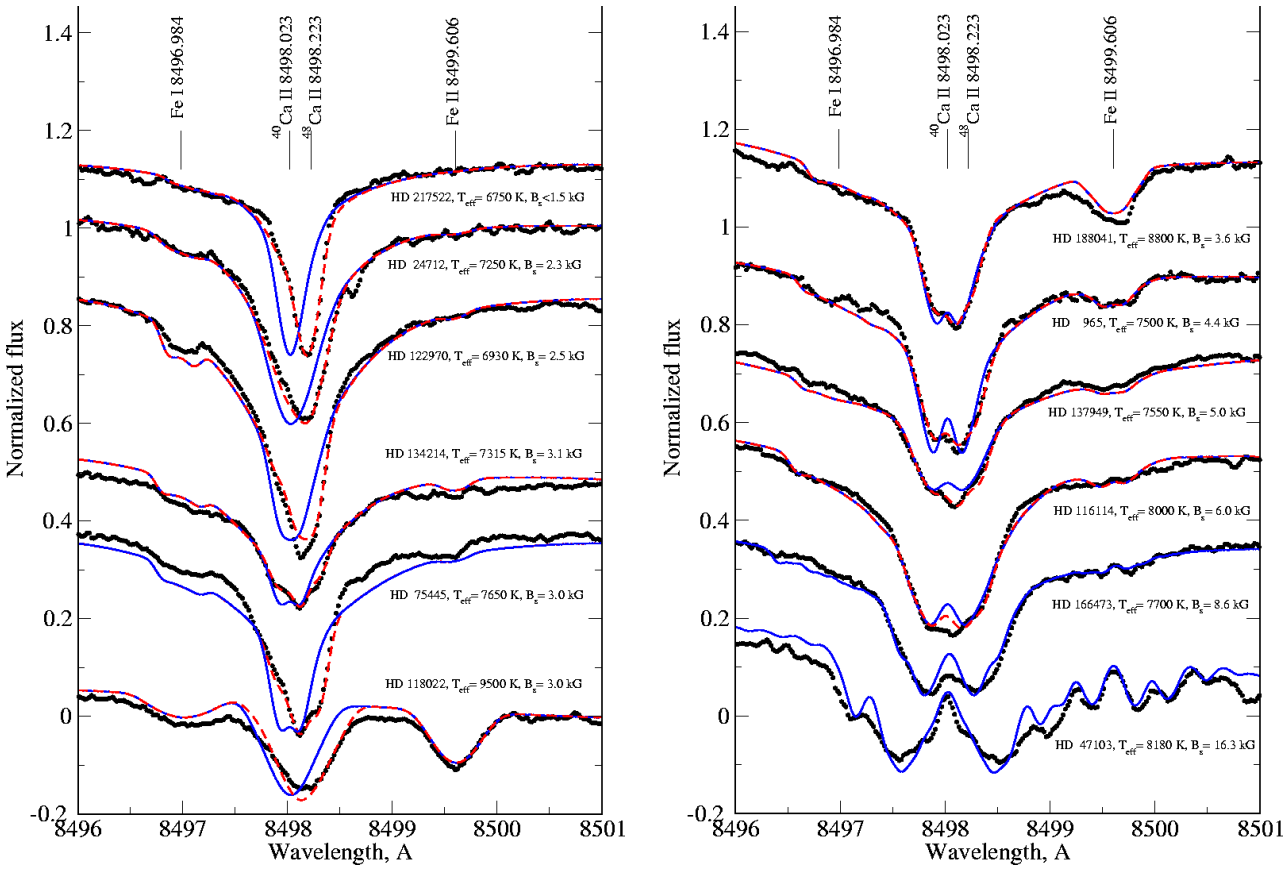

Fig. 9. Comparison of the observed (full circles) and calculated (lines) profiles of the Ca II 8498 Å line in a subset of program stars. Solid line shows theoretical calculations for the terrestrial Ca isotopic mixture and the Ca stratification derived from optical lines. The dashed line presents spectrum synthesis for the models with vertical separation of the Ca isotopes. The stars are arranged in order of increasing magnetic field strength.

field strength. In stars with more intense fields heavy Ca isotopes tend to accumulate much higher in the stellar atmospheres (Fig. 11b). There is also an anticorrelation of the heavy Ca contribution and the total equivalent width of the Ca II 8498 Å transition (Fig. 11c), which implies that the efficiency of the isotope separation process depends on the total line intensity in cases where such separation exists.

We find no difference between roAp and non-pulsating Ap stars (shown with different symbols in Fig. 11) regarding the presence of heavy Ca excess in their atmospheres and its correlation with the magnetic field strength and line intensity.

8. Discussion and conclusions

In this paper we have investigated the vertical stratification and isotopic anomaly of Ca in a large sample of cool magnetic Ap stars. Our study is the first to address the interesting problem of the presence of heavy Ca isotopes in chemically peculiar stars with detailed polarized radiative transfer calculations, which take into account the effects of the magnetic field and chemical separation in stellar atmospheres. We derive stratification of Ca for 23 Ap stars using a sample of Ca I and Ca II lines distributed over a broad spectral range. All but one program stars clearly show signatures of the Ca stratification, whereas comparison stars reveal no inhomogeneities in the vertical Ca distribution when analysed with the same techniques and atomic data. Although our stratification modelling was based on a simplified step-function approximation and adopted a simplified homogeneous model for the magnetic field geometry, the inferred parameters of the vertical Ca distributions impose important observational constraints for theoretical models of the radiative diffusion processes in stellar atmospheres.

Analysis of the IR Ca triplet line Ca II 8498 Å provided information on the relative contribution of different Ca isotopes. Spectrum synthesis calculations show that significant isotopic shifts observed in the core of Ca II 8498 Å cannot be attributed to the overabundance of heavy Ca isotopes throughout the whole stellar atmosphere. Instead, we show that the Ca line profile shape is consistent with the vertical separation of different Ca isotopes, with heavy Ca located in a cloud above the most abundant isotope ^{40}Ca. Even though the presence of heavy Ca is prominent in the line core, the normal Ca isotope dominates the line wings and is more abundant in the lower atmosphere where the total Ca abundance is also much larger. Thus, our tentative model calls for a less extreme heavy Ca enrichment than was suspected in previous investigations limited to the centroid measurements of the Ca II 8498 Å line core.

Recently different stratification of He isotopes was found by Bohlender (2005) in the analysis of ^{3}He and related stars. That paper used a similar approach to modelling chemical stratification, but has only addressed He vertical distribution in hot non-magnetic chemically peculiar stars.

We have successfully used the model with Ca stratification and vertical isotopic separation to explain the appearance of the Ca II 8498 Å in all stars showing excess of heavy Ca isotopes. The prominent anticorrelation between the presence of heavy

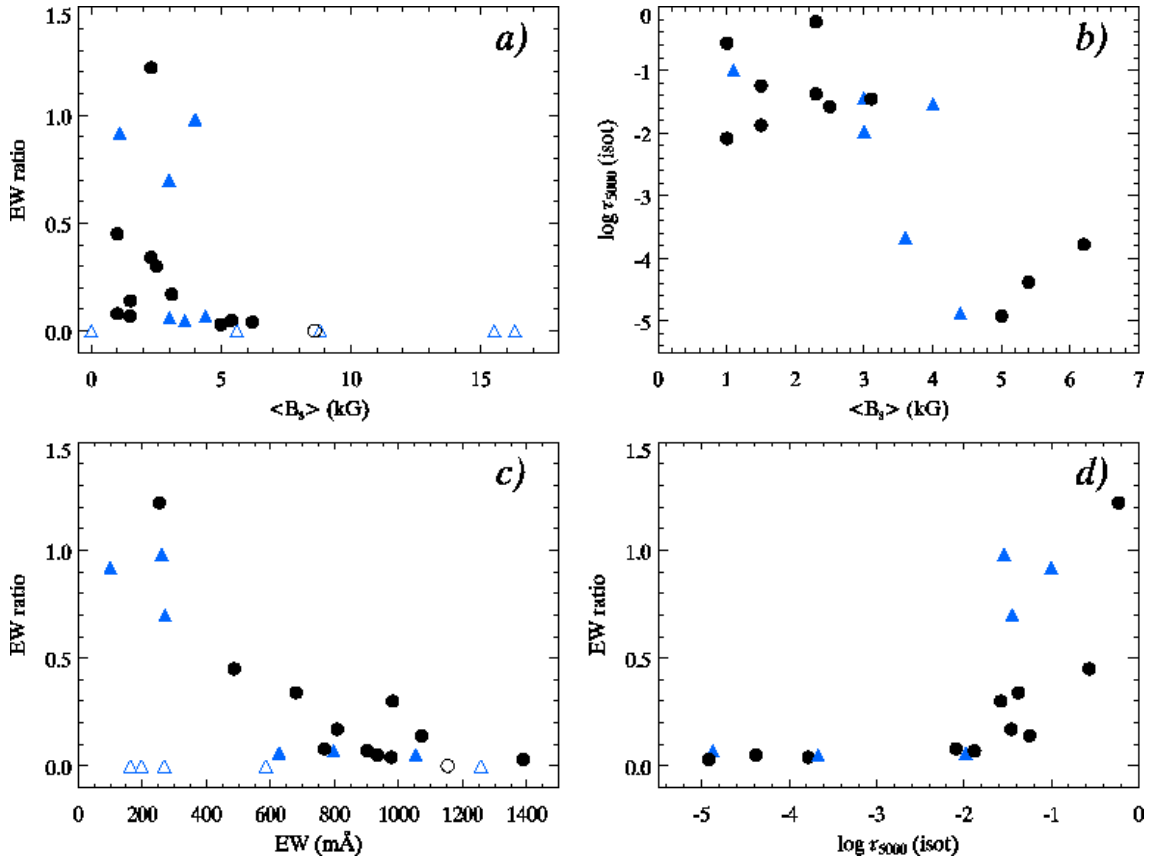

Fig. 11. Results of the analysis of Ca isotopic composition in Ap stars. **a)** ratio of calculated equivalent width of the heavy and light Ca components of the 8498 Å line vs. magnetic field strength. **b)** Position of the boundary between the light and heavy Ca layers vs. magnetic field strength. **c)** The equivalent width ratio vs. the total equivalent width of the Ca II 8498 Å line. **d)** The equivalent width ratio vs. the optical depth of the boundary between the light and heavy Ca layers. In all plots different symbols correspond to Ap stars with detected presence of heavy Ca (*filled symbols*) and those showing no heavy Ca isotopes (*open symbols*), as well as to roAp (*circles*) and non-pulsating Ap (*triangles*) stars.

Ca and magnetic field strength, first reported by Ryabchikova (2005), is confirmed and strengthened in the present paper. We find that only stars with sufficiently weak field show traces of heavy Ca. According to our knowledge, this interesting relation is the only case when definite dependence of the chemical abundance characteristic on the magnetic field strength is found for Ap stars. Furthermore, we find that in stars with stronger fields the heavy Ca isotopes tend to accumulate higher in the atmosphere.

According to the results of our study, pulsating (roAp) and non-pulsating Ap stars are not distinguished by the characteristics of their Ca isotopic anomaly. Both groups of stars are equally likely to show an excess of heavy Ca and follow the same trend of the heavy isotope contribution versus the magnetic field strength and the Ca II 8498 Å line intensity.

If the overall distribution of Ca abundance in the atmospheres of Ap stars follows the predictions of the radiatively driven diffusion, our results on the isotopic separation favour the light-induced drift (LID) as the main process responsible for this separation. According to Atutov & Shalagin (1988), LID arises when the radiation field is anisotropic inside the line profile. Such an anisotropy takes place for a line of the trace isotope, for instance ^{46}Ca and ^{48}Ca in the terrestrial calcium mixture, which is located in the wing of a strong line of the main isotope ^{40}Ca. The main isotope induces the drift velocity for other isotopes. If the trace isotope's line is located in the red wing of the line due to main isotope, the drift velocity is directed towards the upper atmosphere and the trace isotopes are pushed upwards. This is in agreement with observed vertical distribution of Ca isotopes. The Zeeman splitting changes the line shape and decreases the flux anisotropy for the line of trace isotope. When magnetic field becomes strong enough, ~5–6 kG, the flux anisotropy disappears and the isotopic separation is ceasing. Therefore, the observed Ca isotopic anomaly in magnetic stars may be qualitatively explained by the combined action of the radiatively-driven diffusion and the light-induced drift. Theoretic study of a combination of the radiatively-driven diffusion and LID was presented by LeBlanc & Michaud (1993) for He. These authors showed that LID accelerates separation of ^{3}He from ^{4}He in hotter CP stars. Detailed theoretical chemical diffusion calculations (LeBlanc & Monin 2004) should incorporate LID in order to test our hypothesis that this effect may be important for the chemical transport processes in cool Ap-star atmospheres.

Acknowledgements. We thank Luca Fossati for letting us use his spectrum of HD 73666. This work was supported by the RAS Presidium Program "Origin and Evolution of Stars and Galaxies", by Austrian Science Fund (FWF-P17580N2) and by the grant 11630102 from the Royal Swedish Academy of Sciences. TR also acknowledges partial support from the RFBR grant 06-02-16110a and the Leading Scientific School grant 162.2003.02. OK acknowledges financial support from the Swedish Royal Physiographic Society in Lund.

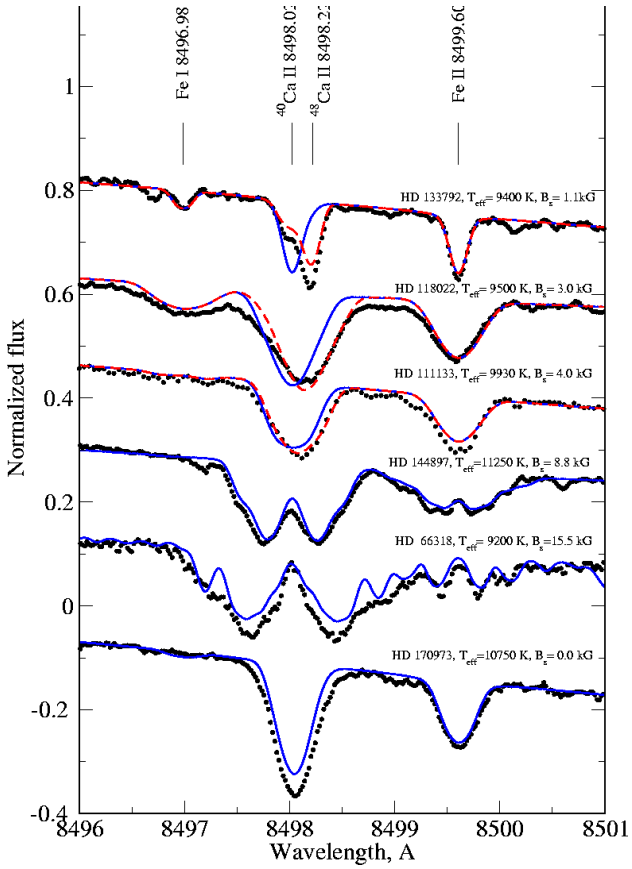

Fig. 10. Same as in Fig. 9 but for the stars with $T_{\rm eff}$> 9000 K.

References

Allende Prieto, C., Asplund, M., Garćia Lopez, R.J., & Lambert, D. 2002, ApJ, 567, 544
Anders, E., & Grevesse, N. 1989, Geoch. Cosmochim. Acta, 53, 197
Atutov, S. N., & Shalagin, A. M. 1988, Astron. Letters, 14, 284
Babel, J. 1992, A&A, 258, 645
Babel, J. 1994, A&A, 283, 189
Bagnulo, S., Wade, G.A., Donati, J.-F., et al. 2001, A&A, 369, 889
Bagnulo, S., Jehin, E., Ledoux, C., et al. 2003a, Messenger, 114, 10
Bagnulo, S., Landstreet, J. D., Lo Curto, G., Szeifert, T., & Wade, G. A. 2003b, A&A, 403, 449
Ballester, P., Modigliani, A., Boitquin, O., et al. 2000, Messenger, 101, 31
Barklem, P. S., Piskunov, N., & O'Mara, B. J. 2000, A&A, 393, 1091
Bohlender, D. 2005, in *Element Stratification in Stars: 40 Years of Atomic Diffusion*, eds. G. Alecian, O. Richard and S. Vauclair, EAS Publ. Ser., 17, 83
Borsenberger, J., Michaud, G., & Praderie, F. 1981, ApJ, 243, 533
Castelli, F., & Hubrig, S. 2004, A&A, 421, L1
Cowley, C. R., Ryabchikova, T., Kupka, F., et al. 2000, MNRAS, 317, 299
Cowley, C. R., & Hubrig, S. 2005, A&A, 432, L21
Cowley, C. R., Hubrig, S., & Kamp, I. 2006, ApJS, 163, 393
Cowley, C. R., Hubrig, S., Castelli, F., Gonzalez, J. F., & Wolff, B. 2007, MNRAS, 377, 1579
Dappen, W., Anderson, L., & Mihalas, D. 1987, ApJ, 319, 195
Dekker, H., D'Odorico, S., Kaufer, A., Delabre, B., & Kotzlowski, H. 2000, proc. SPIE, 4008, 534
Dimitrijević, M.S., & Sahal-Bréchot, S. 1993, JQSRT, 49, 157
Fossati, L., Bagnulo, S., Monier, R., Khan, S.A., Kochukhov, O., Landstreet, J., Wade, G., & Weiss, W. 2007, A&A, 476, 911
Gelbmann, M., Kupka, F., Weiss, W. W., & Mathys, G. 1997, A&A, 319, 630
Gelbmann, M. 1998, Contrib. Astron. Obs. Scalnaté Pleso, 27, 280
Gelbmann, M., Ryabchikova, T. A., Weiss, W. W., Piskunov, N., Kupka, F., & Mathys, G. 2000, A&A, 356, 200
Glagolevskii, Yu. V., Ryabchikova, T. A., & Chountonov, G. A. 2005, Astron. Letters, 31, 327
Hauck, B., & Mermilliod, M. 1998, A&AS, 129, 431
Hubeny, I., Hummer, D. G., & Lanz, T. 1994, A&A, 282, 151
Kato, K. 2003, PASJ, 55, 1133
Kochukhov, O. 2007a, in *Magnetic Stars 2006*, eds. I.I. Romanyuk and D. O. Kudryavtsev, Nizhnij Arkhyz, p.109
Kochukhov, O. 2007b, in *CP#Ap Workshop*, eds. J. Žižňovský, J. Zverko, E. Paunzen, M. Netopil, Contribut. Astr. Obs. Skalnaté Pleso, in press (astro-ph/0711.4908)
Kochukhov, O., Landstreet, J.D., Ryabchikova. T., Weiss, W.W., & Kupka, F. 2002, MNRAS, 337, L1
Kochukhov, O., & Bagnulo, S. 2006, A&A, 450, 763
Kochukhov, O., & Wade, G. A. 2007, A&A, 467, 679
Kochukhov, O., Tsymbal, V., Ryabchikova, T., Makaganyk, V., & Bagnulo S. 2006a, A&A, 460, 831
Kochukhov, O., Freytag, B., Piskunov, N., & Steffen, M. 2006b, in *IAU Symposium No. 239, Convection in Astrophysics*, eds. F. Kupka, I.W. Roxburgh, K.L. Chan, 68 (astro-ph/0610111)
Kupka, F., Ryabchikova, T. A., Weiss, W. W., Kuschnig, R., Rogl, J., & Mathys, G. 1996, A&A, 308, 886
Kurucz, R. L. 1993, CDROMs 13,22,23, SAO, Cambridge
Landstreet, J. D. 1998, A&A, 338, 1041
LeBlanc, F., & Michaud, G. 1993, ApJ, 408, 251
LeBlanc, F., & Monin, D. 2004, in *The A-Star Puzzle*, IAU Symp. 224, eds. J. Zverko, W.W. Weiss, J. Žižňovský, S.J. Adelman, 193
Leone, F., Vacca, W. D., & Stift, M. J. 2003, A&A, 409, 1055
Lüftinger, T., Kochukhov, O., Ryabchikova, T., Weiss, W.W., & Ilyin, I. 2007, in *Physics of Magnetic Stars*, eds. I.I. Romanyuk and D. O. Kudryavtsev, 119
Mårtensson-Pendrill, A.-M., Ynnerman, A., Wartson, H., et al. 1992, Phys. Rev., A45, 4675
Mashonkina, L., Korn, A. J., & Przybilla, N. 2007, A&A, 461, 261
Mathys, G., Hubrig, S., Landstreet, J. D., Lanz, T., & Manfroid, J. 1997, A&AS, 123, 353
Michaud, G. 1970, ApJ, 160, 641
Michaud, G., Richer, J., & Richard, O. 2005, ApJ, 623, 442
Moon, T. T., & Dworetsky, M. M. 1985, MNRAS, 217, 305
Napiwotzki, R., Schönberner, D., & Wenske, V. 1993, A&A, 268, 653
Nielsen, K., & Wahlgren, G. M. 2002, A&A, 395, 549
Nörtershäuser, W., Blaum, K., Icker, P., et al. 1998, Eur. Phys. J., D2, 33
Rogers, N. Y. 1995, Comm. in Asteroseismology, 78
Ryabchikova, T. 2005, in *Element Stratification in Stars: 40 Years of Atomic Diffusion*, eds. G. Alecian, O. Richard and S. Vauclair, EAS Publ. Ser., 17, 253
Ryabchikova, T. A., Landstreet, J. D., Gelbmann, M. J., Bolgova, G. T., Tsymbal, V. V., & Weiss, W. W., 1997, A&A, 327, 1137
Ryabchikova, T. A., Savanov, I. S., Hatzes, A. P., Weiss, W. W., & Handler, G. 2000, A&A, 357, 981
Ryabchikova, T., Piskunov, N., Kochukhov, O., Tsymbal, V., Mittermayer, P., & Weiss, W. W. 2002, A&A, 384, 545
Ryabchikova, T., Leone, F., Kochukhov, O., & Bagnulo, S. 2004a, in *The A-Star Puzzle*, IAU Symp. 224, eds. J. Zverko, W.W. Weiss, J. Žižňovský, S.J. Adelman, 580
Ryabchikova, T., Nesvacil, N., Weiss, W. W., Kochukhov, O., & Stütz, Ch., 2004b, A&A, 423, 705
Ryabchikova, T., Leone, F., & Kochukhov, O. 2005, A&A, 438, 973
Ryabchikova, T., Ryabtsev, A., Kochukhov, O., & Bagnulo, S. 2006, A&A, 456, 329
Savanov, I. S., Kochukhov, O. P., & Tsymbal, V. V. 2001, Astrophysics, 44, 206
Seaton, M. J., Mihalas, D., & Pradhan, A. K. 1994, MNRAS, 266, 805
Smith, G. 1988, J. Phys., B21, 2827
Smith, G., & Gallagher, A. 1966, Phys. Rev., 145, 26
Smith, G., & O'Neil, J. A. 1975, A&A, 38, 1
Smith, G., & Raggett, D.St.J. 1981, J. Phys., B14, 4015
Stehlé, C., & Hutcheon, R. 1999, A&AS, 140, 93
Theodosiou, C.E. 1989, Phys. Rev. A39, 4880
Wade, G. A., LeBlanc, F., Ryabchikova, T. A., & Kudryavtsev, D.O. 2003, in *Modelling of Stellar Atmospheres*, IAU Symp. 210, eds. N.E. Piskunov, W.W. Weiss and D.F. Gray, D7